Advances in Forest Fire Research

Domingos Xavier Viegas

EDITOR

2014

Fine fuel particle heating during experimental laboratory fires

Jack D. Cohen, Mark A. Finney

[a] *US Forest Service, Missoula Fire Sciences Laboratory, Missoula, MT 59808 USA*
jcohen@fs.fed.us, mfinney@fs.fed.us

Abstract

Fuel particle temperature measurements were related to measurements of particle irradiance and impinging gas temperatures during seven fire spread experiments at the U.S. Forest Service Fire Sciences Laboratory, Missoula, Montana. Fine particle temperature increases corresponded to pulses of impinging hot gases and thus suggested convection as the primary heat transfer mechanism responsible for particle ignition. An analysis using the flux-time product correlation (FTP) indicated that flame radiation was insufficient to pilot ignite fuels for fire spread. A numerical modeling examination of fine particle heating indicated flame radiation was insufficient for particle ignition and convection heat transfer from flame contact was the primary heating mechanism leading to particle ignition.

Keywords: Fuel heating, Fire spread, Ignition processes

1. Introduction

Since the 1940's wildfire spread has been described as a step-wise process of ignition by heat transfer from the burning zone to adjacent fine fuel particles (Fons 1946). Observations and experiments have identified fine live and dead vegetation (e.g. conifer needles and twigs < 3 mm diameter) as the burning fuels primarily responsible for the intensity of the propagating flame zone and thus wildfire spread (Fons 1946; Rothermel 1972; Pagni and Peterson 1973; Call and Albini 1997; Stocks *et al*. 2004). For example, after fire spreads through shrub and tree canopies the branches larger than 6 mm commonly remain unconsumed after a high intensity wildfire has burned the area. Thus, understanding fire spread requires an understanding of ignition processes at spatial and temporal scales of fine fuels.

Sufficient understanding of wildland fire spread processes does not exist for reliable *ex ante* physical modeling. An indicator of this insufficient understanding is the inconsistency between fire spread models that attempt physical descriptions of radiation and convection (Sullivan 2009). Model developers have largely assumed fuel particle ignition processes without an experimental basis (Finney *et al*. 2013a). For example, radiation heat transfer has been commonly assumed to govern fire spread. However, experimental evidence suggests radiation heat transfer is insufficient for igniting fine fuel particles (Fang and Steward 1969; Baines 1990; Finney *et al*. 2013a). And prior experimental evidence (Rothermel and Anderson 1966; Fang and Steward 1969) and laboratory fire observations (Baines 1990; Fang and Steward 1969) indicated that most fuel particle heating to ignition occurred within the last 0.025 m during fire spread. Given that burning fine fuels are primarily responsible for wildland fire spread, if radiation is insufficient for fine fuel ignition then convection must be the heat transfer mechanism governing fire spread. The convective heating would occur from flame impingement on fuels adjacent to the flaming front, and recent experiments have shown how this occurs (related paper[1]). The following discussion describes measured fuel particle temperatures related to measured incident radiation heat fluxes (irradiance) and gas temperatures during experimental surface fires and how that relates to heat transfer mechanisms governing fire spread.

---

[1] Finney et al. 2014. Experimental evidence of buoyancy controlled flame spread in wildland fires; VII ICFFR.

2. Methods

We are experimentally examining wildfire ignition processes to provide a basis for physically modeling fire spread. The following discussion describes fuel particle heating experiments with measurements made at fine fuel particle spatial and temporal scales. The experiments relate measured fine fuel particle temperatures with measured irradiance and impinging gas temperatures during the approach of spreading flame zones. In conjunction with the experiments, heat transfer processes are examined using modeling.

2.1. Experiments

Special wood fuel particles were instrumented with thermocouples along with measurements of incident radiation (irradiance) and gas temperatures adjacent to the particles. Machined wood (*Liriodendron tulipiferia*) particles with 1 mm and 12 mm square cross-sections, both 120 mm long were instrumented with fine thermocouples (K Type, 0.05 mm). The 1 mm fuel particles had thermocouples embedded at the center of the front (facing the approaching flames) and back vertical surfaces; the 12 mm particles had thermocouples embedded at the center of each vertical and horizontal surface (front, top, back and bottom) (Figure 1). The fuel particles were horizontally attached to the top of precisely constructed cardboard "comb" fuel beds. The particles were located 130 mm to one side of the center line of the 2.44 m wide fuel bed in the U.S. Forest Service experimental wind tunnel burning facility in Missoula, Montana.
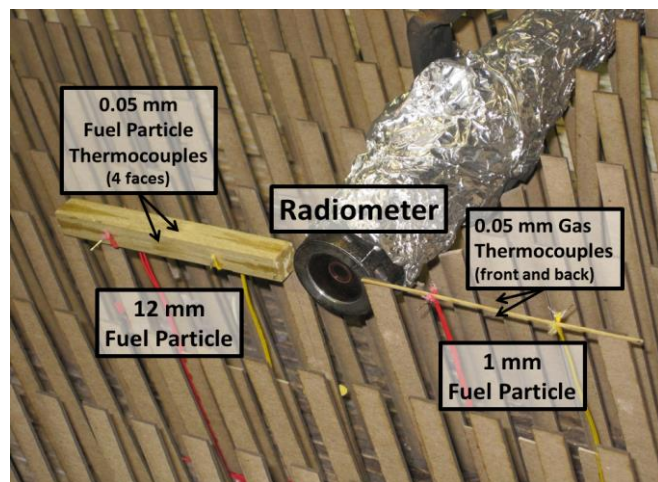

Figure 1 - 1 mm and 12 mm fuel particles were instrumented with 0.05 mm thermocouples. The 1 mm particle had thermocouples embedded in the centers of front and back faces only; the 12 mm particle had thermocouples centered in four faces (ends are neglected). The particles were attached to the top of a "fuel comb" in the cardboard fuel bed. The comb fuel bed shown had tines 152 mm tall and 12.4 mm wide and spaced 46 mm between rows. A water cooled radiometer at fuel particle height estimated particle irradiance and suspended 0.05 mm thermocouples estimated gas temperatures.

Fuel particle irradiance and temperatures of impinging gases were measured as the fire spread to the particles. Fuel particle irradiance was estimated using a water-cooled radiometer placed even with the fuel particles. Temperatures of gases flowing around the fuel particles were estimated using fine thermocouples (K Type, 0.05 mm) suspended approximately 5 mm from the particle's front and back vertical faces (Figure 1). To reliably measure the flame radiation we calibrated the radiometer using a black body cavity having temperatures in the range of a spreading flame front (1000 K – 1400 K). All measurements were taken at a sampling rate of 500 per second (500 Hz). At this rate, the sampling time interval (.002 sec) is less than one-half the time constant (.04 sec) of the fastest responding sensor (thermocouple) and meets Nyquist frequency aliasing criteria (Fritschen and Gay 1979). Measurements began before fuel bed ignition and continued through fine particle ignition and burning.

The "comb" fuel beds were engineered using 1.25 mm thick cardboard (Finney *et al*. 2013b). Each comb was laser cut from a 1.2 m long sheet to specified tine heights and widths (Figure 1). Fuel particles were mounted on combs having tine widths of 2.31 mm, 6.20 and 12.4 mm and comb heights ranging from 102 mm to 203 mm. To change flame zone characteristics fuel beds were constructed with combs at various spacing widths between rows and combinations of combs with different tine

heights and widths. For fuel beds with comb size combinations, fuel particles were mounted on the combs with the highest tines.

2.2. Modeling

We used a two-dimensional numerical model of fuel particle heat transfer to further examine particle heating during the fire experiments. The numerical model calculates fuel particle temperatures across the particle mid-section and these temperatures reasonably represent temperatures for most of the particle. This assumes that end effects are negligible and the particle exchanges energy uniformly along its length (120 mm) such that no significant lengthwise temperature gradients occur through most of the particle. The numerical model used a finite difference, explicit method with a grid increment of 2.5×10^{-5} meters between computational nodes and a time increment of 5.0×10^{-4} seconds. We verified that the computational results were stable and independent of spatial and temporal increments. The irradiance and gas temperature measurements from the experiments were used as inputs to the 1 mm particle model.

The initial conditions and boundary conditions were determined by a combination of measured values and assumed values. We assumed the fuel particle initially had uniform temperature corresponding to the measured front face temperature before heating from the flame front. It was assumed the particle was in equilibrium with its surroundings just prior to the first model computation. Radiation boundary conditions were estimated by the measured irradiance for the front face and the designated constant blackbody temperature of the surroundings for the other three faces of the particle. The convection boundary conditions were estimated by a computed convection heat transfer coefficient and the measured gas temperature adjacent to the fuel particle front face. For the lack of a convection coefficient correlation that matched the particle heating context, the Hilpert average correlation for non-circular forms (Incopera and DeWitt 2002) was used. The flow velocities were assumed based on the measured gas temperature. At gas temperatures below 500 C the flow velocity was designated to be the wind tunnel flow speed. For gas temperatures equal to and greater than 500 C, the gas flow velocity was increased to seven times the ambient flow based on observations of higher flow circulations associated with flames. Although the convection coefficient and air properties were determined for the entire particle based on the average film temperature for the front face, the heat transfer was calculated at each computational node. At every time increment, the physical properties of the wood particle were determined by the temperature at each computational node.

The model only accounted for heat exchange and did not include chemical kinetics and mass transfer related to moisture vaporization and pyrolysis. Although particles were not oven-dried prior to the experiments, the 1 mm particles had moisture contents less than six percent and assumed negligible for modeling. Pyrolysis was assumed negligible at particle temperatures below 275 C. The model was considered unreliable at temperatures above 275 C and thus modeling ended prior to particle ignition. The purpose of the modeling was to examine heat transfer processes leading to particle ignition during fire spread. There was no intent to develop a predictive tool with this effort. Thus, model parameters were set without benefit of prior comparisons between model and experimental results and model parameters were not adjusted after comparisons to improve estimates of measured particle temperatures.

3. Results

Seven fire spread experiments were conducted with instrumented fuel particles. To describe the context of the particle heating experiments related to fire conditions, Table 1 provides the wind speed, fire spread rate, flame length, flame zone depth and particle irradiance for each burn. After ignition the experimental fires spread with a nearly straight flame front across the 2.44 meter wide fuel bed. The flame lengths from Table 1 suggest fire characteristics similar to those burning actual fuel beds composed of short grasses or surface forest litter under dry conditions and low wind speeds. The factors contributing to the variety of spread rates and flame lengths such as fuel bed characteristics are beyond the scope of this discussion and not included in the Table 1.

Table 1. Laboratory Fire Spread Conditions. Wind speed was a constant wind tunnel setting. Rate of spread and flame length were estimated after the influence of the ignition line became negligible. Flaming depth was the estimated distance from the forward edge of the propagating flame front to the rear where coherent flaming ceases due to fuel consumption. The fuel particle irradiance range is from the last four seconds before the 1 mm particle ignition.

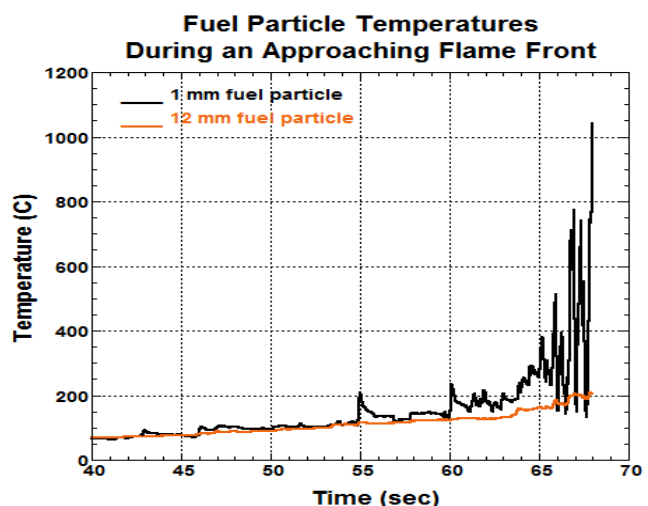| Fire Exp.	Wind Speed (m/s)	Rate of Spread (m/s)	Flame Length (m)	Flaming Depth (m)	Irradiance [4 s to ign.] (kW/m^2)
a	0.34	0.028	1.0	0.54	20 - 29
b	0.34	0.024	1.2	0.41	20 - 30
c	0.22	0.016	1.4	0.57	22 - 40
d	0.56	0.032	1.2	0.68	17 - 34
e	0.34	0.031	1.3	0.56	25 - 44
f	0.67	0.034	1.5	0.60	13 - 22
g	0.34	0.03	0.6	0.28	10 - 22

Every experiment produced the same general results regarding the fuel particle thermal response to transient conditions and ignition. The 1 mm particles responded quickly to changing thermal conditions compared to the 12 mm particles (Figure 2). Within the last four seconds of the approaching flame front the 1 mm particle temperatures rapidly increased resulting in sustained ignition while the 12 mm particle had not yet ignited before flame front arrival (Figure 2). Particle ignition was determined by fuel particle and gas temperatures and confirmed with video recordings. In all seven experiments the 1 mm particles ignited before the 12 mm particles.

None of the experiments produced measured fuel particle irradiance capable of piloted ignition. Using a validated irradiance based ignition correlation (Cohen 2004) the flux-time product (FTP) was computed from the measured fuel particle irradiances. The resulting FTP values for all the fuel particle experiments were well below the criteria for ignition. For example, the maximum measured irradiance of the fuel particle experiments was 44 kW/m^2 (Table 1, experiment "e") and the FTP value when the 1 mm particle sustainably ignited was 1313. The minimum value for piloted ignition is 11501, nearly an order of magnitude greater (Figure 3). Thus, radiation heat transfer was insufficient for particle ignition during all the fire spread experiments.

We take a closer examination of fine fuel heating during an approaching flame front. Because the general response characteristics of all fuel particle heating experiments were similar, we use measurements from fire experiment "d" (Table 1) to show the 1 mm particle response related to the irradiance and gas temperatures.

Figure 2 - For the same thermal conditions, the 1 mm particle (black) has a large temperature variation compared to the 12 mm particle (orange). In the last second of data the 1mm particle ignited while the 12 mm particle had not yet reached a temperature corresponding to a pyrolysis rate that could result in piloted ignition (example from

Examination of the 1 mm particle response uses measurements of the irradiance, gas temperatures adjacent to and in front of the fuel particle and front face surface particle temperature ("front" refers to the side facing the fire). The 1 mm particle temperature graph (Figure 4) starts before significant thermal exposure from the flame front and ends just prior to the 1 mm particle ignition. Gas temperatures (blue) less than the particle temperature (black) indicate convective cooling; gas temperatures higher indicate convective heating. The gas temperature chronology shows intermittent high temperature spikes for approximately 20 seconds prior to ignition whereas radiant flux increases more steadily. Radiation energy absorbed by the particle is indicated by

Figure 3 - The FTP (solid black) is calculated based on the measured irradiance (red, from experiment "e"). If the minimum FTP for ignition (broken black) is met and

particle temperatures remaining higher than gas temperatures with noticeable particle temperature responses to gas temperature. Pulses of higher gas temperatures result in particle temperature increases. The higher the gas temperature and longer the pulse duration the greater the particle temperature increase. For example, the particle remains at 100 C – 120 C in the 50 – 55 second time interval (Figure 4). Small temperature increases occur only during pulses of gas temperatures above the particle temperature. The significant particle temperature increases occur during impinging pulses of hot gasses such as those that occur at 55, 60 and 64 seconds (Figure 4). In the last 1.5 seconds of the heating sequence the particle temperature increases from below 200 C and approaches 300 C (with subsequent ignition) only after gas temperatures remain above and several hundred degrees Celsius higher than particle temperatures (Figure 4).

Importantly, the pulsing higher gas temperatures result from the spreading flame front; the wind tunnel air flow is temperature controlled. The pulsing occurred in all fire experiments and produced particle heating downwind of the flame front. In Figure 4 pulses greater than 100 C began at about 20 seconds before particle ignition. Using the average rate of spread for experiment "d" from Table 1 (0.032 m/s) and neglecting the pulse advection time, the flame front was about 0.64 meters (0.032 m/s x 20 s) from the fuel particle when this convective particle heating occurred. The high temperature gas pulses at 55 seconds and 60 seconds (graph times; Figure 4) were greater than 600 C and within the range of visible flame temperatures. These pulses could have been observed as lateral extensions of the non-steady flaming front contacting the fuel particle across distances of 0.35 meters and 0.19 meters, respectively.
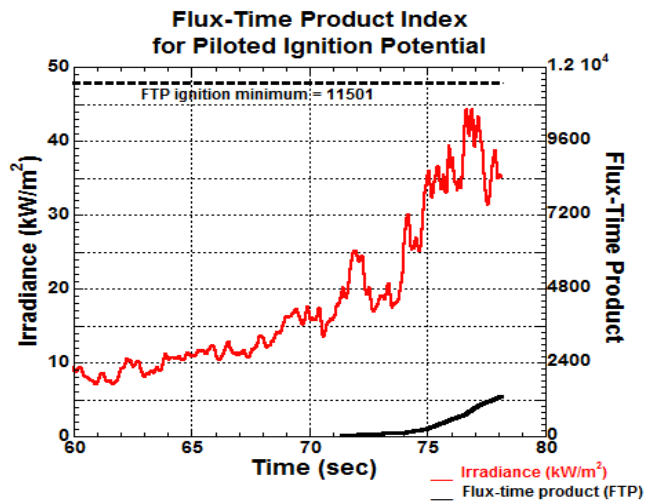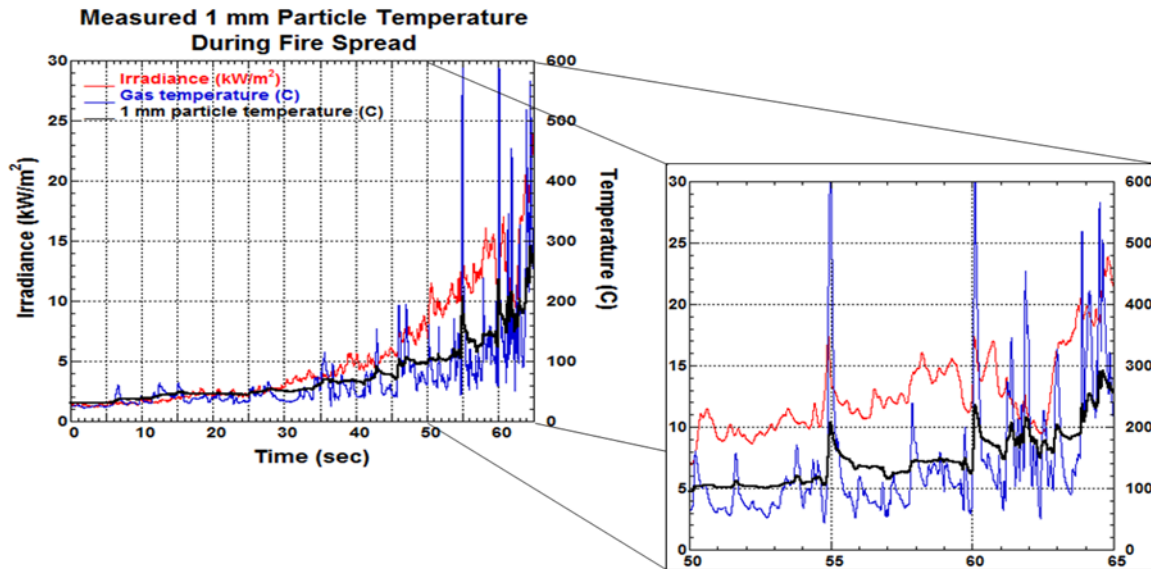
Figure 4. The left graph shows the measured front surface 1 mm fuel particle temperature with the corresponding measured irradiance and front face gas temperature as the fire spread to the particle. The graph ends just prior to particle ignition. The right graph is an enlargement of the last 15 seconds. The right graph shows particle temperatures responding (heating and cooling) to the variations in gas temperature and heating primarily during the pulses of high gas temperatures. (Data from experiment "d" of Table 1.)

The fuel particle heat transfer model computes fuel particle temperatures similar to the measured particle temperatures (Figure 5). Inspection of Figure 5 indicates the model captures the convective heating, both the response time and the magnitude during the high temperature gas pulses at 55 seconds, 60 seconds, and in the last second of the graph. However, the model did not simulate the thermal sensitivity revealed in the measured particle temperatures.
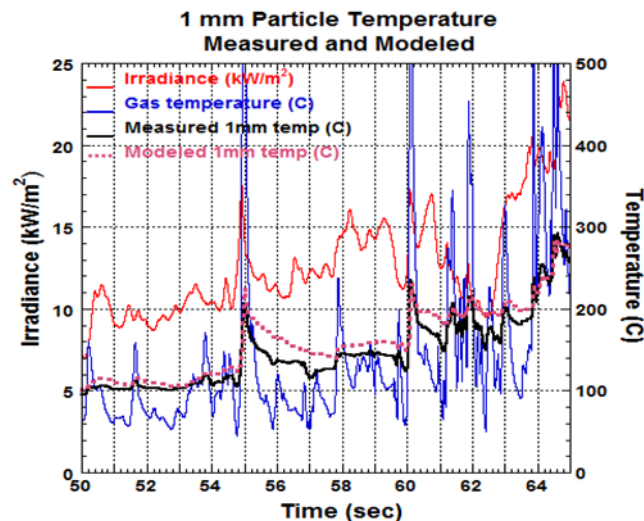

Figure 5. The same measured irradiance and gas temperatures as in Figure 4 are used as inputs for computing the 1 mm particle face temperature (purple). The measured 1 mm face temperature (black) is presented for comparison with the modeled temperature (the last 15 seconds as in the right graph of Figure 4).

In particular, the model does not cool as much as the particle as indicated by the modeled temperature (purple) largely remaining above the particle temperature. It is not clear what factors are causing the

difference but it could be the use of an average particle convection coefficient, higher absorbed radiation than actual and/or measurement errors.

4. Discussion and Analysis

The fuel particle heat transfer experiments have shown the importance of convection heat transfer. As seen in Figure 2 fine fuel particles convectively exchange heat at a higher rate than coarser particles. Thus, at cooler gas temperatures fine fuel particles will more effectively reduce radiation heating but at high gas temperatures fine particles will more effectively heat to ignition. Initially convective cooling was indicated by the particle temperatures largely staying above the gas temperatures (0 − 35 seconds, Figure 4). As the flame front approached (after 35 seconds), fuel particle temperatures increased primarily in response to convection heat exchange and this was particularly evident in the last 1.5 seconds of the graph (Figure 4). A separate analysis using the flux-time product (FTP) correlation based on the measured irradiance indicated insufficient flame irradiance for piloted ignition and thus the necessity of convective particle heating seen in Figure 4. However, even with fine scale sampling during the particle heating experiments it is difficult to differentiate the radiation and convection heat transfer mechanisms during fire spread. A heuristic examination using computational modeling has the potential to overcome practical limits of experimentation and explore questions such as "What if we stopped the flame radiation without affecting flame convection at the particle and vice versa?".

We used the model to examine the specific contributions of flame radiation and flame convection on fuel particle temperature by eliminating one and then the other.

No flame radiation: The measured irradiance was replaced by the constant irradiance of 300 K (27 C) blackbody surroundings. The measured gas temperatures were used as previously modeled. Inspection of Figure 6 indicates the modeled particle temperature responds to gas temperatures similar to the measured particle.
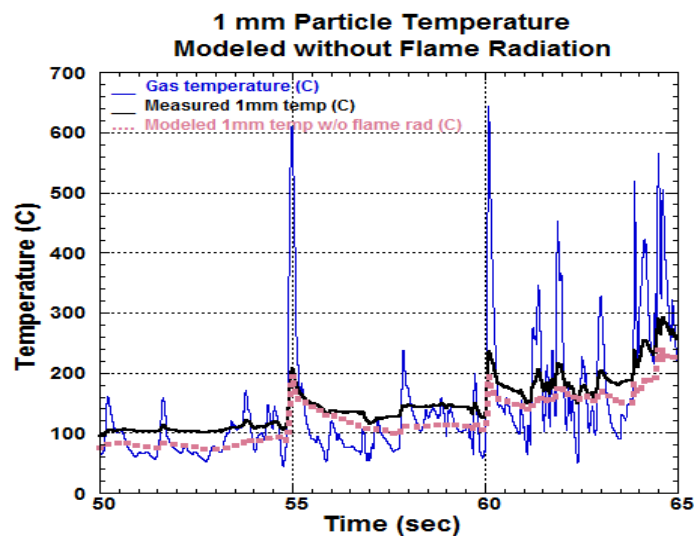

Figure 6. A constant irradiance of 300 K surroundings was substituted for the measured flame irradiance. The measured gas temperatures (blue) were used to compute convection heat transfer as before. The last 15 seconds of the computed particle temperature (purple) was compared to the measured particle temperature (black).

However, without flame radiation the modeled particle temperature remains below the measured temperature and below the modeled temperature in Figure 5. *No flame convection*: The measured gas temperatures were replaced by the constant wind tunnel flow speed of 0.56 meters/second at a constant temperature of 300 K (27 C). The measured irradiance was used as previously modeled. Inspection of

Figure 6 indicates a dramatic change in the modeled particle response characteristics compared to the measured particle.

The rapid increases in measured particle temperatures corresponding to 55 seconds and 60 seconds (Figure 7 graph time) did not occur with the modeled particle. At 63 seconds the modeled particle temperature drops corresponding to the measured irradiance but the measured particle temperature increased.
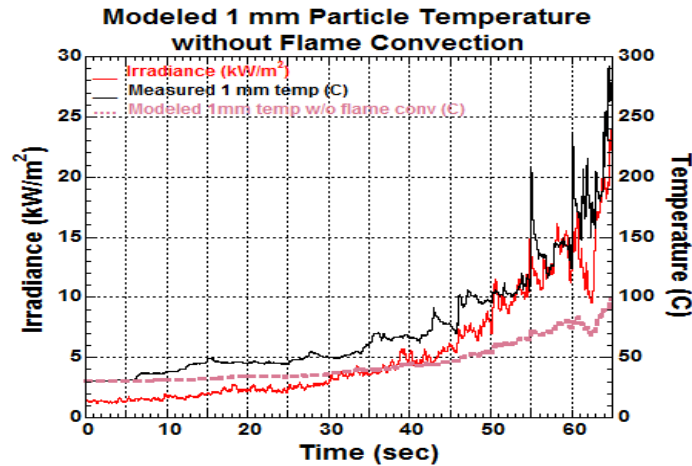

Figure 7. A constant 300 K gas flow was substituted for the flame gases. The measured flame irradiance was used as before. The 65 second sequence shows how the measured particle temperature (black) diverges from the computed temperature (purple) without hot flame gases.

Notably, just prior to ignition the final modeled particle temperature was about 100 C while the measured particle temperature was approaching 300 C. This result is consistent with the FTP analysis indicating that the irradiance was nearly an order of magnitude less than necessary for piloted ignition.

5. Conclusion

Fuel particle heat exchange experiments and heuristic modeling have demonstrated convection heat transfer as the principal mechanism governing fire spread during experimental laboratory fires. Temperature measurements have shown that fine fuel particles thermally respond at the time scales of significant convective pulses. As the flame front approaches, fine particles primarily heat convectively with increasing gas temperatures and pulse frequencies. In agreement with prior research, our experiments showed that the primary heating to ignition of the fine particles occurred within 0.05 meters of the approaching flame front during our laboratory fires. Measured temperatures along with modeling indicate convection heat transfer from flame contact was the primary mechanism responsible for the rapid particle temperature increases prior to particle ignition.

6. References

Baines PG (1990) Physical mechanisms for the propagation of surface fires. *Mathematical Computer Modelling* **13**(12), 83-94.

Call PT, Albini FA (1997) Aerial and surface fuel consumption in crown fires. *International Journal of Wildland Fire* **7**(3): 259-264.

Cohen, JD (2004) Relating flame radiation to home ignition using modeling and experimental crown fires. Canadian Journal of Forestry Research **34**(8): 1616-1626.

Fang JB, Steward FR (1969) Flame spread through randomly packed fuel particles. *Combustion and Flame* **13**, 392-398.

Finney MA, Cohen JD, McAllister SS, Jolly WM (2013a) On the need for a theory of wildland fire spread. *International Journal of Wildland Fire* **22**, 25-36.

Finney MA, Forthofer JD, Grenfell IC, Adam BA, Akafuah NK, Saito K (2013b) A study of flame spread in engineered cardboard fuel beds, Part I: Correlations and Observations. August 6-9, 2013, Seventh International Symposium on Scale Modeling, Hirosaki, Japan.

Fons WL (1946) Analysis of fire spread in light forest fuels. *Journal of Agricultural Research* **72**(3):93-121.

Fritschen LJ, Gay LW (1979) 'Environmental Instrumentation.' (Springer-Verlag: New York)

Incopera FP, DeWitt DP (2002) 'Fundamentals of Heat Transfer and Mass Transfer.' 5th Edition (Wiley: New Jersey)

Pagni PJ, Peterson TG (1973) Fire spread through porous fuels. *Fourteenth Symposium (International) on Combustion* **14**(1): 1099-1107.

Rothermel RC, Anderson HE (1966) Fire spread characteristics determined in the laboratory. USDA For. Serv. Res. Pap. INT-30.

Rothermel RC (1972) A mathematical model for predicting fire spread in wildland fuels. USDA For. Serv. Res. Pap. INT-115.

Stocks BJ, Alexander ME, Wotton BM, Stefner CN, Flannigan MD, Taylor SW, Lavoie N, Mason JA, Hartley GR, Maffey ME, Dalrymple GN, Blake TW, Cruz MG, Lanoville RA (2004) Crown fire behavior in a northern jack pine-black spruce forest. *Canadian Journal of Forestry Research* **34**: 1548-1560.